The Role of Compliant Elements in Two-Legged Robot's Foot Model

Submitted: 24th October 2014; accepted: 22nd December 2014

Magdalena Sylwia Zurawska, Teresa Zielinska, Maksymilian Szumowski

DOI: 10.14313/JAMRIS_1-2015/9

Abstract:

Proposition of compliant foot for bipedal robot is introduced and its properties are investigated. The foot consists of four compliant elements (spring-damper) mounted to four vertices of a rectangular frame. The results of robot gait analysis using Zero Moment Point method are shown. ZMP trajectories for rigid and compliant foot are compared and conclusions are formulated. Foot compliance reduces needed for postural stabilization compensatory movements of the upper part of the body by those simplifying control methods and construction. Obtained results will be applied in real prototype of small humanoidal robot. Robot construction in which proposed foot will be applied is shortly introduced.

Keywords: *humanoidal robots, compliance, ankle joint, robotic feet, prototyping*

1. Introduction. Motivations

There is seen an important trend in today's robotic: newly developed robots more often move fast and naturally like the animals. This trend is especially visible in humanoidal robots – they imitate people not only by their appearance but also by their motion. This is visible in robots constructed at Waseda University [5]. To achieve similarities between robot and human, not only appropriate mechanical body structure, control system and motion pattern are needed but also the proper foot-ground contact must be assured. Such contact can be obtained by the phenomenon of mechanical compliance. In the past the robot parts including robot's feet were usually made out only of a stiff components. Today more often compliant elements are applied. They are not only used as a separate components, but they create complex compliant mechanical systems where several compliant elements interact with each other. Robot described in [4] is such an example – it is jumping robot with compliant bio-inspired legs. RunBot robot [6] is the robot with a flat feet and actively powered ankle joint. Robot design was inspired by the human bone structure. RunBot is claimed to be well stable when moving over undulating terrain. In the paper [7] a robot with multiple-segmented actively powered foot is proposed. Authors [7] tested their model in terms of achievable gait velocity. It was shown that velocities in knee joints might be reduced while maintaining the same gait velocity.

As it is illustrated by Fig. 1 there are two main methods of introducing compliance into robotic feet: – passive way exploiting compliant materials and spring-damper systems – active way with powered compliant joints. The benefit of passive way is simplicity and low weight because this solution does not need the actuation and not any control. Active compliance has no such advantages but the behaviours exceeding those offered by passive compliance can be achieved. Therefore the selection of passive or active compliance must be carefully investigated taking into account the final aim of the whole robot.

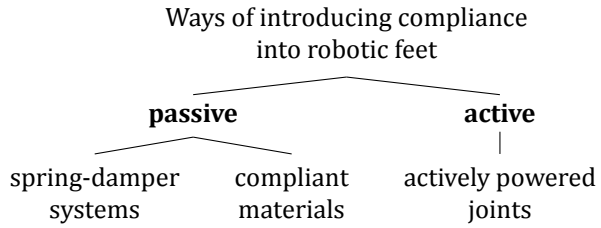

Fig. 1. Introducing compliance into robotic feet

Passive compliant elements used in the robotic feet can be considered as an equivalent of the foot arch (Fig. 2) which decreases the body impacts in human gait.

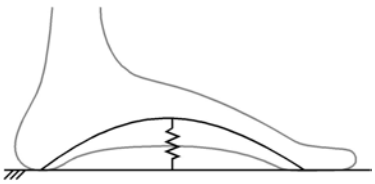

Fig. 2. Human foot arch acting as an impacts damper

Together with positional adjustment, foot arch assures the low-impact contact with the ground, it also supports take-off impulse on the beginning of the transfer phase [5].

There is the research [1], [13], [14] on compliant structures conducted by our group. Simple model of the foot with one spring located near to the ankle joint was proposed and applied in small humanoid (Fig. 3). Conducted by us theoretical and experimental studies confirmed that the proposed simple compliant structure improves the postural stability. Applied structure absorbed the landing impact however, because of the lack of frontal compliance, take-off impulse was not achieved. Applied only one spring was offering only the planar compliance (human foot arch due to the foot width is a 3 dimensional system). Such limitation

motivated us to the studies on the new concept of compliant foot introduced in this paper.

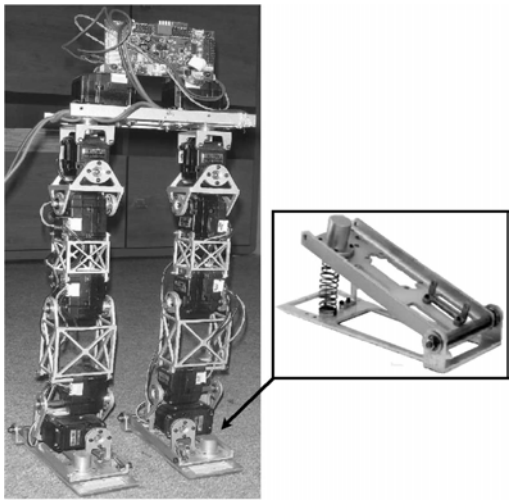

Fig. 3. First version of compliant foot and the robot where it was applied

2. Foot Model

Developing the foot we considered its future application. The biped in which the feet will be used is small and lightweight. The robot was designed in such way that the moments powering the legs in transfer are possibly small. It was assumed that not all degrees of freedom will be actuated. Actuators add unnecessary weight to the robot's lower extremities what results in increasing the actuating moments demands. This is especially critical for not powering the robot displacement leg transfer phase. It was the additional motivation for using passive spring-damper systems in our robot's feet. As it was mentioned, our previous research [14] confirmed that passive compliance improves the postural stability. New concept of the robotic foot exploits the advantages of the previous structure.

New foot model is made of two stiff layers with four compliant elements between them (Fig. 4). The elements are located in four vertices of the rectangular frame and each of them consists of a spring and damper. Their properties are described by the well known formula:

$$c_j \dot{z}_j + k_j z_j = F_j \tag{1}$$

where c_j is the damping factor of the j-th compliant element ($j = A, B, C, D$), k_j stands for the spring stiffness of j-th element, F_j is a part of the force applied on the j-th element, z means compression. It must be noted that every element can have different stiffness or different damping. Dimensions of the foot were chosen with accordance to anthropometric data of the typical adult man, that means – the foot length 0.30 m, and width 0.10 m. The system was analyzed for constant orientation of the foot (the whole sole is touching the ground – full support phase). The compliant element acts only along the z-axis direction which

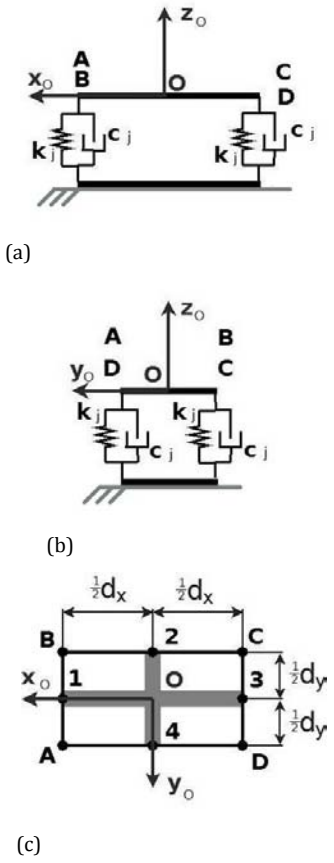

Fig. 4. Concept of the robot foot

is perpendicular to the ground. System is attached to the ankle joint like a human foot. Distortion of compliant elements influences the body posture – compliant elements are compressed due to the acting forces. As it will be explained in the next section, such changes are influencing the postural stability.

Additional conditions Considered system is statically undetermined so to analyze its properties the additional conditions must be introduced. In our case they result from axial symmetry of the foot – the point O (point where the ankle joint is located, Fig. 5) lies in the middle of rectangular foot frame.

The total vertical force F ($F = \sum_i m_i \ddot{z}_i + \sum_i m_i g$, where g is gravitational constant and m_i is the mass of i-th segment of the body – see section 3) applied to ZMP point P' is equilibrated by the reaction force F_r ($F_r = -F$). Force F can be distributed to F_A, F_B, F_C, F_D – four components acting to the foot edges (see Fig. 5). Those forces produce compressions of foot's compliant elements. Such compressions, if different, produces the sway of the foot upper layer (Fig. 5), what results in the sway of overall body. Such change of posture affects the position of ZMP (section 3, Eq. (13a),(13b)). Therefore, for postural analysis F_A, F_B, F_C and F_D must be known. The virtual works principle was applied to evaluate those forces.

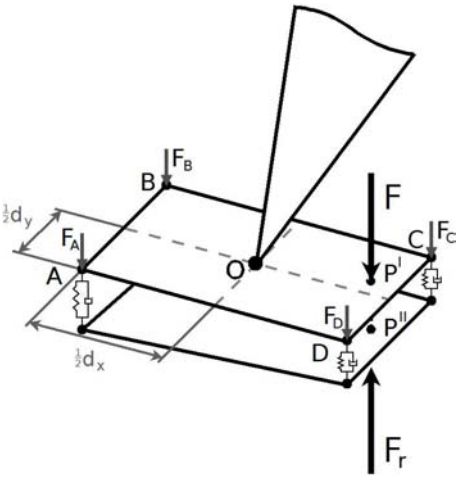

Fig. 5. Schematic view of the foot

Virtual works principle The principle of virtual works [9] is based on energy balance of mechanical system. Net change of internal energy (δL) caused by small displacement have to be equal to the difference between work output and input ($\delta W = W_{out} - W_{in}$) to this system.

When system is in equilibrium under given forces and an arbitrary small displacement $\delta\mathbf{r}$ occurs, the net change in internal energy δL will equal the work (δW) done on the system: $\delta L = \delta W$. Virtual work (δW) is the one that is generated by the virtual force $\mathbf{F}^{(v)}$ acting on appropriate virtual displacement $\delta\mathbf{r}$. Virtual work is a scalar value, measured in work/energy units:

$$\delta W = \mathbf{F}^{(v)} \cdot \delta\mathbf{r} = \delta L \tag{2}$$

Virtual work of a system consisting of n force-displacement components is expressed by:

$$\delta W = \sum_{k=1}^{n} \mathbf{F}_k^{(v)} \cdot \delta\mathbf{r}_k \tag{3}$$

Determining the forces One of many practical applications of the virtual works principle is obtaining reaction forces in beams. To use this method, foot model was simplified to the set of two beams (Fig. 4c): one beam considered in xz-plane supported in points 1 and 3 (Fig. 6a) and second beam considered in yz-plane supported in points 2 and 4 (Fig. 6b). Such simplification allows us to determine forces in points 1, 2, 3 and 4 using virtual works principle. With F_1, F_2, F_3 and F_4 known, F_A, F_B, F_C and F_D forces can be easily obtained.

Beam shown in Fig. 7 is released in point 3. Then, according to the *Virtual Works Principle*, small displacement occurs in this point. There are two forces: F – total vertical force, and $R_3 = -F_3$ (Fig. 7) – reaction force applied to point 3, and two displacements: δp and δr_3 respectively. Force F can appear on two sides of the point O (Fig. 7). In considered system forces act only along z-axis.

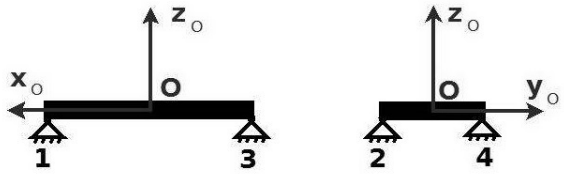

(a) (b)

Fig. 6. Foot model considered as two beams

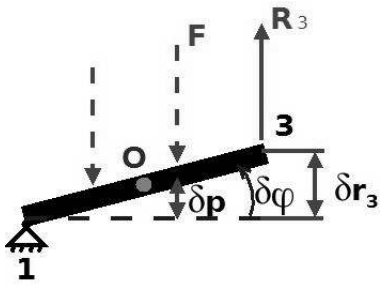

Fig. 7. Beam released in point 3. Dotted lines illustrate that the force F can be applied to any point on the beam

In our case Eq. (3) takes the form:

$$R_3\delta r_3 - F\delta p = -F_3\delta r_3 - F\delta p = \delta L = 0 \tag{4}$$

The system is in balance so the net energy change is zero $\delta L = 0$. In Eq. (4) force F is known.

Considered system has 1 degree of freedom. φ is our generalized variable. As it was mentioned before, principle of virtual works assumes small displacements, what means that $sin(\delta\varphi) = \delta\varphi$. We obtain:

$$\delta r_3 = d_x \sin(\delta\varphi) \tag{5a}$$

$$\delta r_3 = d_x\delta\varphi \tag{5b}$$

and:

$$\delta p = \left(\frac{d_x}{2} \pm {d_x}^{ZMP}\right)\delta\varphi \tag{6}$$

The distance from point O to the point where force F is applied is denoted by ${d_x}^{ZMP}$ and as it was mentioned can be located on both sides of the point O. Centre of footprint is located in distance $\frac{1}{2}d_x$ from the point 1 (Fig. 8). So force F acts in distance $\frac{1}{2}d_x \pm {d_x}^{ZMP}$ from the point 1.
Substituting Eq. (5b) and Eq. (6) into Eq. (4) and rearranging the terms we get:

$$\left(-F_3 d_x - F\left(\frac{d_x}{2} \pm {d_x}^{ZMP}\right)\right)\delta\varphi = 0 \tag{7}$$

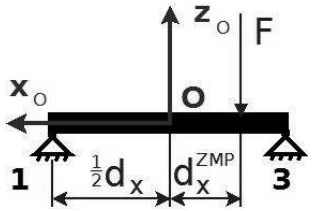

Fig. 8. Distances dependencies: d_x, ${d_x}^{ZMP}$

When the system is in balance, generalized force by which $\delta\varphi$ is multiplied in Eq. (7) is equal to zero:

$$\left(-F_3 d_x - F\left(\frac{d_x}{2} \pm {d_x}^{ZMP}\right)\right) = 0 \tag{8}$$

Using Eq. (8) F_3 can be directly evaluated:

$$F_3 = -\frac{F}{d_x}\left(\frac{d_x}{2} \pm {d_x}^{ZMP}\right) \tag{9}$$

Analogical procedure is applied in all other cases and F_1, F_2 and F_4 are obtained:

$$F_1 = -\frac{F}{d_x}\left(\frac{d_x}{2} \mp {d_x}^{ZMP}\right) \tag{10a}$$

$$F_2 = -\frac{F}{d_y}\left(\frac{d_y}{2} \pm {d_y}^{ZMP}\right) \tag{10b}$$

$$F_4 = -\frac{F}{d_y}\left(\frac{d_y}{2} \mp {d_y}^{ZMP}\right) \tag{10c}$$

Now we have four forces F_1, F_2, F_3 and F_4 acting in four midpoints (points: $1, 2, 3$ and 4) of the foot edges, but we need four forces F_A, F_B, F_C and F_D acting in four foot vertices (points: A, B, C, D). Assumption of foot axial symmetry allows us to derive F_A, F_B, F_C and F_D. Points 1, 2, 3 and 4 are midpoints, so the distances to the appropriate neighbour points A, B, C, and D are always the same: half of the foot dimensions ($\frac{1}{2}d_x$ or $\frac{1}{2}d_y$) (see Fig. 4c). Due to above, we can assume symmetrical distribution of calculated forces F_i ($i = 1, 2, 3, 4$) to the vertices A, B, C and D.

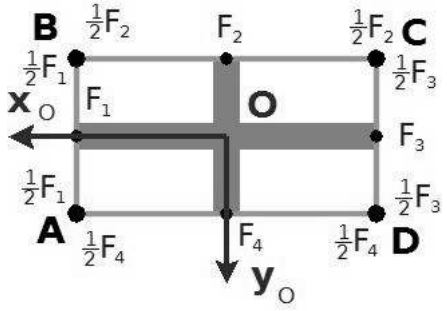

Fig. 9. Schematic illustration of forces distribution

For example, there is force F_2 in point 2. We assign $\frac{1}{2}F_2$ for point B point and the same for C. As it can be seen in Fig. 9 we have 2 forces acting to each vertex, so to find the whole force acting on it we apply:

$$F_A = \frac{1}{2}F_1 + \frac{1}{2}F_4 = \frac{1}{2}(F_1 + F_4) \tag{11a}$$

$$F_B = \frac{1}{2}F_1 + \frac{1}{2}F_2 = \frac{1}{2}(F_1 + F_2) \tag{11b}$$

$$F_C = \frac{1}{2}F_2 + \frac{1}{2}F_3 = \frac{1}{2}(F_2 + F_3) \tag{11c}$$

$$F_D = \frac{1}{2}F_3 + \frac{1}{2}F_4 = \frac{1}{2}(F_3 + F_4) \tag{11d}$$

3. Gait Stability – ZMP Method

The problem of stability criterion for two-legged locomotion was in focus of attention for a long time. In 1968 Vukobratovic introduced the breakthrough method [11] called *Zero Moment Point* method. The method is commonly used in theoretical studies and in practical applications. In this method *Zero Moment Point* indicating if the posture is stable in single support phase is calculated using relations formulated by Vukobratovic or it is obtained in real-time (during walking) based on the measurements.

When evaluating *Zero Moment Point* it is assumed that distributed masses of body segments are represented by properly located point masses. For postural stability during single-support phase it is required that all moments due to the motion dynamics of point masses are equilibrated by the moment due to the reaction force. Therefore, in stable posture, the application point (ZMP point) of reaction force obtained using torques equilibrium condition must stay inside of robot's footprint. The equilibrium condition is considered towards the axes of reference frame attached to the ankle joint (point O). Fig. 10 illustrates the ZMP concept described by Eq. (12):

$$\sum_i (\mathbf{r}_i \times \mathbf{F}_i) + \mathbf{I}_i\dot{\omega}_i + \omega_i \times \mathbf{I}_i\omega_i = -\mathbf{r}_P \times \mathbf{F}_r \tag{12}$$

here $\mathbf{r}_i$ is the position vector of m_i mass and $\mathbf{F}_i$ is the force generated by this mass, $\mathbf{I}_i$ is the inertia matrix, ω_i is the angular velocity, $\mathbf{r}_P$ is the vector from point O to P (ZMP point) – the application point of $\mathbf{F}_r$ – the reaction force. Its coordinates are easily derived by rearranging the M_x and M_y (Fig. 10) torques equilibrium conditions [15]:

$$X_{zmp} = \frac{\sum_i [x_i(m_i\ddot{z}_i + m_i \cdot g)] - \sum_i (z_i \cdot m_i\ddot{x}_i)}{\sum_i (m_i\ddot{z}_i + m_i g)} \tag{13a}$$

$$Y_{zmp} = \frac{\sum_i [y_i(m_i\ddot{z}_i + m_i \cdot g)] - \sum_i (z_i \cdot m_i\ddot{y}_i)}{\sum_i (m_i\ddot{z}_i + m_i g)} \tag{13b}$$

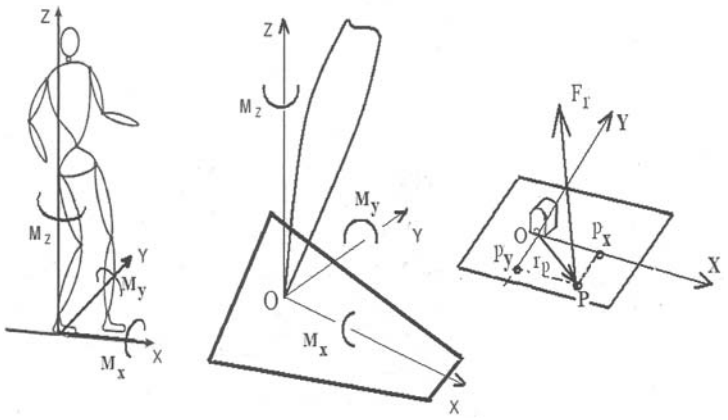

Fig. 10. Idea of* Zero Moment Point *method

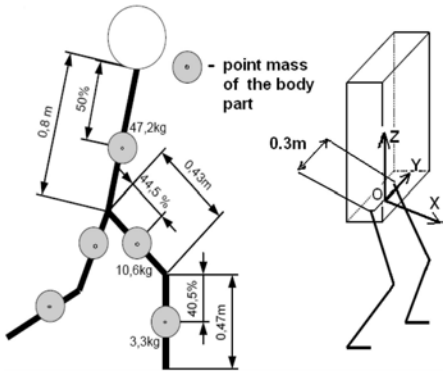

Fig. 11. Robot model

In Eq. (13) x_i, y_i and z_i represent coordinates of i-th mass, while second derivatives of those coordinates $\ddot{x}$, $\ddot{y}$, and $\ddot{z}$ are accelerations. As it is commonly applied, in Eq. (13a) and (13b) some very small but difficult for calculations terms are neglected. By analyzing the ZMP trajectory during support phase we can determine whether the robot's posture is stable or not. Mentioned omission of small components in Eq. (13) results in the requirement that the ZMP trajectory must be located inside the foot-print keeping some distance from the foot boundary.

Investigating the properties of proposed compliant foot we considered human body model taken from [14] illustrated in Fig. 11. This is the model of 50-centile adult man $1.75m$ tall with $75kg$ body mass. The body segments (legs and torso) are represented by the point masses located in segments' center of gravity. All the necessary dimensions and masses are shown in Fig. 11. The model is three-dimensional, the torso can move not only along the walking direction but also can incline to the sides as it is a feature of human locomotion. Considered in our investigations legs' movement (gait pattern) was planar matching the data recorded by human motion tracking system. It must be emphasized that reference to anthropometric data allowed us to compare the obtained results to the results of real human gait. Considered simplified model of the body matches well the robot body build in which the investigated feet will be applied.

4. Gait Pattern

Recorded by us [13] gait pattern was used. Gait was recorded for slow walk of a typical 50-centile man ($1.75m$ tall) using VICON system. This system allows to capture the motion in one plane applying the markers as it is shown in Fig. 12.

Fig. 12. Student prepared for gait recording, markers are the white points

In Fig. 13 recorded gait pattern is presented. There are four angular trajectories, angles are positive when the body segment is before the vertical line and analogically negative when the body segment is after the vertical line which is attached to the adequate joint (see Fig. 13).

5. Tests and Results

Recorded during experiments trajectories where applied as the motion pattern of considered human body model. Point masses accelerations and positions together with overall reaction force were obtained based on recorded trajectories and then ZMP trajectory (Eq. (13)) was calculated. The total vertical force F generated by the robot's body, as mentioned before, is distributed into four forces acting on the foot's vertices. These forces produce compressions of compliant

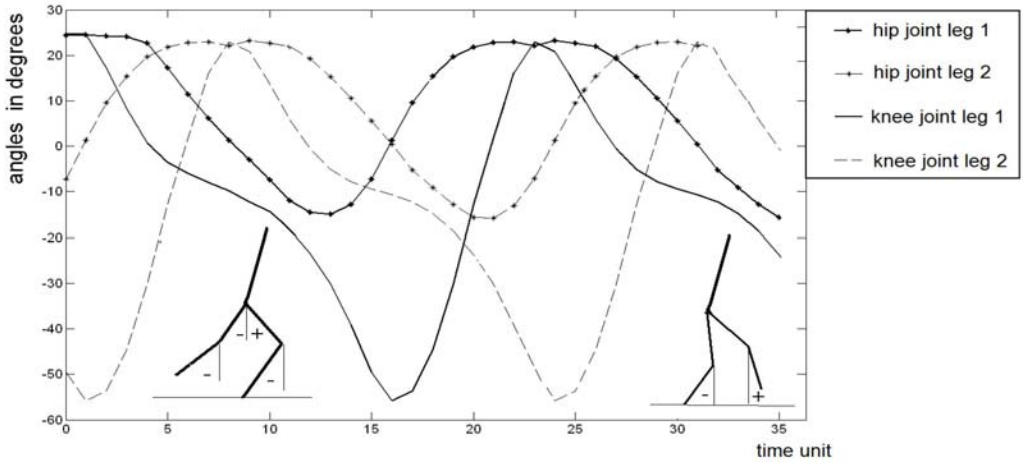

Fig. 13. Gait pattern used in our considerations.

elements. These compressions affect postural stability and the trajectory of ZMP as well. Compressions z_j are calculated using Eq. (1) and forces F_j ($j = A, B, C, D$) are calculated according to Eq. (11).

Results presented in this paper (Fig. 14) concern the single-support phase of a right leg (results for the left leg are analogical). The ZMP trajectory obtained for the model with rigid feet was considered as the reference. The ZMP trajectories for the compliant feet with different compliance and stiffness were analyzed. Their comparison to reference trajectory answered the question if compliance improves the body stability. Comparative study of the ZMP trajectories obtained for different stiffness and damping indicated what set of parameters is the most appropriate.

During preliminary studies for a stiff leg, the ZMP trajectory exceeded the area of the footprint. It meant that the compensatory movements of upper part of the body were needed as it is in human walking. During human gait torso sways to sides (left, right) up to 8^o to each side. Our three dimensional model allowed us to introduce such movement, so it was added. Such motion is also commonly applied in humanoids [3]. With swaying torso in this range, the ZMP trajectory went inside the footprint so the postural stability was achieved. Then the compliant foot model was applied and it was noticed that the compensatory trunk movements should be decreased – the required range of sway was small (in range of 3^o to each side). Such result confirmed that the passive compliant elements in the feet are substituting actively powered swaying of the trunk.

According to the diagrams (Fig. 14) in both cases (stiff leg, compliant leg) the y coordinate (across the foot) of ZMP decreases fast on the beginning of the single-support phase – the ZMP moves from outer side of the footprint towards the center, to the line crossing the projection of the ankle joint (point with $y = 0$). In this fragment of support phase the ZMP is in the rear towards the ankle (x coordinate is negative). Later the ZMP does not moves much to the side of footprint (y is almost constant) but displaces to the front

(a)

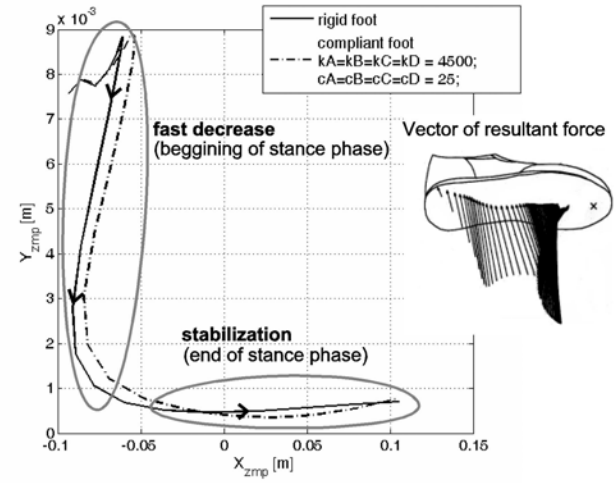

(b)

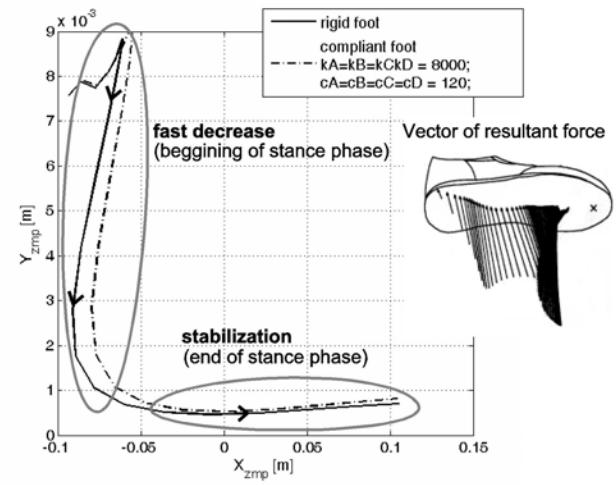

Fig. 14. ZMP trajectories for different parameters of compliant elements. For the comparison the ZMP trajectory recorded during human walking is shown.

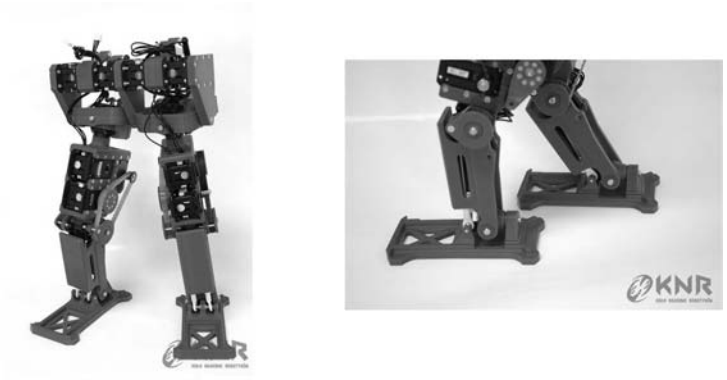

(a) (b)

Fig. 15. Prototype of small biped

(x coordinate increases). Comparing the ZMP trajectories for rigid and compliant foot it can be noticed that with compliance the first part of ZMP trajectory is smoother and the trajectory is shifted more to the front in the first phase of support (x coordinate is a bit bigger). It means that the ZMP for the compliant foot is located further from the rear end of the footprint what is very desirable: postural stabilization is better because the whole system can comply with bigger disturbances.

Comparison between ZMP trajectories for compliant foot with different parameters indicated that better correction is achieved with higher values of spring stiffness (Fig. 14).

6. Small Biped

As it was mentioned, the research on foot compliance has in aim its application in our prototype shown in Fig. 15, [10]. It was decided to imitate human joints with biggest motion ranges, what results in robot's 12 degrees of freedom (two in the ankle joint, one in the knee and three in each hip). This well mirrors the human body properties, thereby anthropometry of this robot was achieved. Main axes of the hip joint are located in such way that they intersects in one point, what is exactly the feature of a human hip joint (Fig. 16).

In the legs the motion from the actuators is transmitted to the joints using parallel structures. Those structures supports the legs mass reduction allowing to locate the actuators closely to the trunk. It decreases the energy needed for legs transfer. Feet are changeable using simple fixing mechanism located in the ankle joint. The foot mounting is shown in Fig. 17. It allows easily attach any new foot for testing.

7. Conclusions

Presented approach will be used for compliant feet design and for robot motion synthesis. Our final aim is to deliver the methods for the design of small, lightweight autonomous bipeds. Such constructions must be simple and with the lightweight feet what is important for energy savings.

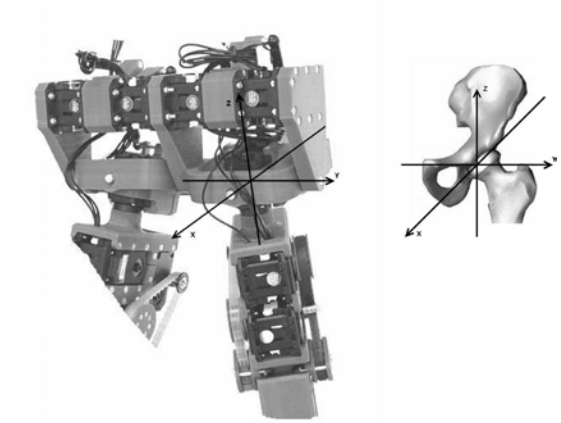

Fig. 16. Robot and human hip joints

Fig. 17. Illustration of the foot mounting

It must be also noted that with more centered localization of ZMP trajectory obtained with compliant foot the robot can comply with bigger external disturbances without loosing the postural stability, therefore the proper adjustment of such trajectory is crucial for the gaits over undulating surfaces.

Selection of parameters describing compliant elements must be carefully performed. The wrong choice can bring either no effect or can cause problems with robot's postural stabilization. The active range of the spring used in compliant elements must be taken into consideration. If the spring is more stiff, the trajectory of ZMP in compliant system is more similar to the tra-

jectory for the rigid foot. When decreasing the stiffness the compressions of the elements are bigger – the body sways more what can finally result in loosing the postural stability.

Needed for postural stabilization trunk movements were replaced by the work of passive compliant elements in the feet (Fig. 18). It is a big advantage because it simplifies the mechanical design and control strategy decreasing the amount of control signals and motion transmission systems through smaller number of needed actuators.

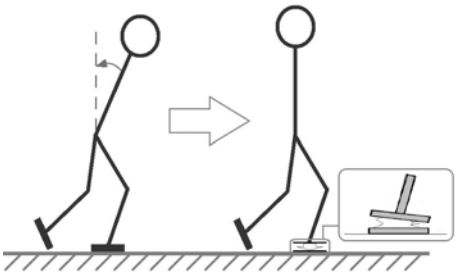

Fig. 18. Compliant feet substitute the compensatory trunk movements

ACKNOWLEDGEMENTS

Research on motion dynamics with compliance has been supported by the National Science Center grant no. DEC-2012/07/B/ST8/03993, the work on robot prototype was supported by Warsaw University of Technology Rector's Grant 2011 and 2012 and the work on manuscript was supported by statutory funds.

AUTHORS

Magdalena Sylwia Zurawska – Institute of Aeronautics and Applied Mechanics, Faculty of Power and Aeronautical Engineering, Warsaw University of Technology, Nowowiejska 24, Warsaw, 00-665, e-mail: mzurawska@meil.pw.edu.pl, www: http://tmr.meil.pw.edu.pl/index.php?/pol/Pracownicy/Magdalena-Zurawska.

Teresa Zielinska – Institute of Aeronautics and Applied Mechanics, Faculty of Power and Aeronautical Engineering, Warsaw University of Technology, Nowowiejska 24, Warsaw, 00-665, e-mail: teresaz@meil.pw.edu.pl, www: http://tmr.meil.pw.edu.pl/index.php?/pol/Pracownicy/Teresa-Zielinska.

Maksymilian Szumowski – Institute of Aeronautics and Applied Mechanics, Faculty of Power and Aeronautical Engineering, Warsaw University of Technology, Nowowiejska 24, Warsaw, 00-665, e-mail: mszumowski@meil.pw.edu.pl, www: http://tmr.meil.pw.edu.pl/index.php?/pol/Pracownicy/Maksymilian-Szumowski.

REFERENCES

[1] Alba González A., Zielinska T., *Postural Equilibrium Criteria Concerning Feet Properties For Biped Robots*, "Journal of Automation, Mobile Robotics & Intelligent Systems" 2012, vol. 6, No. 1, 22–27.

[2] Bruneau O., Ben Oezdou F.:, "Compliant contact of walking robot feet". In: *Proc. of ECPD International Conference on Intelligent Robotics, Intelligent Automation and Active Systems*, 1997, 1–7.

[3] Bum-Joo L., Yong-Duk'K., Jong-Hwan K., "Balance control of humanoid robot for HuroSot". In: *Proc. of* 16^{th} *IFAC World Congress*, 2005, vol. 16, part 1, 2087–2092.

[4] Ganesh K. K., Pushparaj Mani P., "Dynamic modelling & simulation of a four legged jumping robot with compliant legs", *Robotic and Autonomous Systems*, 2013, vol. 61, 221–228.

[5] Hashimoto K. et al., "A Study of Function of Foot's Medial Longitudinal Arch Using Biped Humanoid Robot", 2010 IEEE/RSJ International Conference on Intelligent Robots and Systems, 2010, 2206–2211. DOI: 10.1109/IROS.2010.5650414.

[6] Manoonpong P. et al., "Compliant Ankles and Flat Feet for Improved Self-Stabilization and Passive Dynamics of the Biped Robot "RunBot"", *International Conference on Humanoid Robots*, 2011, 276–281.

[7] Nishiwaki K. et al., "Toe joints that enhance bipedal and fullbody motion of humanoid robots". In: *Proc. of IEEE International Conference on Robotics and Automation, ICRA*, 2002, vol.3, 2277–2282. DOI: 10.1109/ROBOT.2002.1013704.

[8] Sellaouti R. et al., "Faster and Smoother Walking of Humanoid HRP-2 with passive toe joints", In: *IEEE International Conference on Intelligent Robots and Systems*, ICRA, 2006, vol. 1, 4909–4914. DOI: 10.1109/IROS.2006.282449.

[9] Uicker J. J., Pennock G. R., Shigley J. E., *Theory of Machines and Mechanisms*, Third Edition, Oxford University Press, 2003. DOI: 10.1115/1.1605769.

[10] Szumowski M., *Project and Development of Humanoid Robot Prototype. Bachelor of Science Thesis*, The Faculty of Power and Aeronautical Engineering, Warsaw University of Technology, 2014.

[11] Vukobratovic M., Borovac B., "Zero – Moment Point – Thirty Five Years Of Its Life", *International Journal of Humanoid Robotics*, 2004, vol. 1, no. 1, 157–173. DOI: 10.1142/S0219843604000083.

[12] Zhang P. et al., "Adaptive Compliant Control of Humanoid Biped Foot with Elastic Energy Storage". In: *International Conference on Advanced*

Intelligent Mechatronics, Signapore, 2009. DOI: 10.1109/AIM.2009.5229892.

[13] Zielinska T. et al., "Robot gait synthesis using the scheme of human motions skills development", *Mechanism and Machine Theory*, vol. 44, no. 3, 2008, 541–558. DOI: 10.1016/j.mechmachtheory.2008.09.007.

[14] Zielinska T., Chmielniak A., "Biologically inspired motion synthesis method of two-legged robot with compliant feet", *Robotica*, vol. 29, no. 7, 2011, 1049–1057. DOI: 10.1017/S0263574711000300.

[15] Zielinska T., *Walking Machines. Principles, Design, Control and Biological Patterns* Warsaw, Wydawnictwo Naukowe PWN, 2014.

[16] Zurawska M., *Analysis of Compliance in Two Legged Robot. Master Thesis*, The Faculty of Power and Aeronautical Engineering, Warsaw University of Technology, 2014.